RSC Advances

Preparation of a titanium metal electrode with a nitrogen-doped one-dimensional titanium oxide surface layer for the support of catalysts.

Journal:	*RSC Advances*
Manuscript ID:	RA-ART-04-2015-006637.R1
Article Type:	Paper
Date Submitted by the Author:	14-May-2015
Complete List of Authors:	Yamaguchi, Seiji; Chubu University, Biomedical Sciences Khanna, Rohit; Chubu University, Department of Biomedical Sciences Matsushita, Tomiharu; Chubu University, Department of Biomedical Sciences Wang, Ang; Kyushu University, Institute for Materials Chemistry and Engineering; Kyushu University, Ohta, Takehiko; Kyushu University, Naruta, Yoshinori; Kyushu University, Takadama, Hiroaki; Chubu University, Biomedical Sciences

Preparation of a titanium metal electrode with a nitrogen-doped one-dimensional titanium oxide surface layer for the support of catalysts.

Seiji Yamaguchi*, Rohit Khanna, Tomiharu Matsushita, Ang Wang, Takehiro Ohta, Yoshinori Naruta , Hiroaki Takadama

Dr. Seiji Yamaguchi, Dr. Rohit Khanna, Prof. Tomiharu Matsushita, Prof. Tadashi Kokubo, Associate Prof. Hiroaki Takadama.
Graduate School of Biomedical Sciences, Chubu University,1200 Matsumoto cho, Kasugai city, Aichi, 487-8501 (Japan)
E-mail: (sy-esi@isc.chubu.ac.jp)
Dr. Ang Wang, Dr. Takehiro Ohta, Prof. Yoshinori Naruta[#].
Institute for Materials Chemistry and Engineering, Kyushu University, 6-10-1 Hakozaki, Higashi-ku, Fukuoka 812-8581 (Japan)

Present address: Institute for Science and Technology Research, Chubu University, 1200 Matsumoto cho, Kasugai city, Aichi, 487-8501 (Japan)

Keywords
titanium, electrode, titanium oxide, support of catalysts, specific surface area, electrical conductivity

Abstract A Ti metal electrode with nanostructured titanium oxide that possesses high electrical conductivity, large specific surface area and the capacity for supporting catalysts was prepared by a simple solution and heat treatment. A precursor of the electrode that possesses one-dimensional hydrogen titanate, $H_2Ti_3O_7$, 600 nm in thickness was produced by soaking the metal in 5 M NaOH at 60 ºC and subsequently in 0.5 mM HCl solution at 40 ºC. The treated metal had high specific surface area approximately 100 times higher than theoretical flat surface, but its scratch resistance was low. The heat treatment of the hydrogen titanate at 650 º C for 1h under air increased the scratch resistance markedly, but resulted in the development of electric insulated surface layer that was composed of anatase and rutile. In contrast, when heat-treated under N_2 atmosphere, the hydrogen titanate was transformed into anatase containing a small amount of Ti_4O_7, TiN, TiN_xO_{1-x} and Ti_2N, which exhibited a relatively higher electrical conductivity that was in the range of semiconducting materials. It was also shown that the treated metal immobilized 1,1'-ferrocenylbis(phosphonic acid) by forming a Ti-O-P bond and thereby induced a high electric current upon cyclic voltammetry, although the treated metal before the ferrocene modification showed almost no electric current. Thus, the treated Ti metal is expected to be useful as an electrode for various types of electrochemical systems due to its high specific surface area, electrical conductivity and large capacity for supporting catalysts.

1. Introduction

The preparation of electrodes with a high specific surface area, high electrical conductivity and large capacity for supporting catalysts has long been a desired goal in order to achieve maximum efficiency in electrochemical reactions. For instance, it was reported in a water electrolysis system that the use of certain catalysts, such as a Ru complex[1] or a Mn porphyrin system[2] reduces excess electrical potential by suppressing side reactions and thus markedly increases efficiency. It is expected that an electrode that possesses a high specific surface area as well as large capacity for catalyst support would bear a large amount of the catalysts on its surface. Thus, the electrode would exhibit efficient water electrolysis if electrical conductivity between the catalysts and the substrate were sufficiently high.

Titanium oxides with a one-dimensional structure, such as nanowires, nanobelts and nanotubes, afford an attractive means of addressing this issue, since they have a high specific area[3,4] and can immobilize various types of catalysts that have been functionalized with carboxyl or phosphate groups[5,6]. A typical procedure to prepare the electrode with the one-dimensional TiO_2 materials is anodic oxidation of a Ti metal[7]. This method allows the synthesis of TiO_2 nanotube arrays with a tunable shape and size on the substrate surface. However, the TiO_2 nanotubes formed in this way are fragile and easily detached from the metal substrate[8].

In contrast, biomaterial studies reported that a 1 μm-layer consisting of sodium hydrogen titanate, $Na_xH_{2-x}Ti_3O_7$, with a one-dimensional structure was formed on the surface of Ti when the metal was soaked in 5M NaOH solution at 60 ºC for 24 h[8]. The sodium hydrogen titanate was transformed into sodium titanate, $Na_2Ti_6O_{13}$, and rutile by a subsequent heat treatment at 600 ºC for 1 h in air[9,10]. The surface layer thus formed had a graded chemical composition in which oxygen and sodium gradually decreased with increasing depth, and it displayed a high degree of scratch resistance and hence was durable enough for extensive handling, even in surgical operations[11]. It was subsequently found that the sodium hydrogen titanate formed by the NaOH treatment transforms into hydrogen titanate, $H_2Ti_3O_7$, in water or diluted HCl solution by an exchange of sodium ions with oxionium ions, and transforms into the anatase- and rutile-type TiO_2 by additional heat treatment without any evident change in the surface morphology[12,13]. These structural changes of the surfaces of the metal is schematically shown in Figure1. Thus the prepared materials might be useful even for the electrode due to their graded chemical composition, high scratch resistance, and high surface area. However, since the application of these materials has been limited in biomaterials, there are few reports on their electrical conductivity.

In the present study, Ti metal electrodes with nano-structured titanium oxides were prepared by NaOH and HCl treatments along with subsequent heat treatment in air or a nitrogen atmosphere, and their utility in electrochemical systems was investigated in terms of their surface area, electrical conductivity and capacity for catalyst support. The capacity for catalyst support was estimated by the immobilization of 1,1'-ferrocenylbis (phosphonic acids) and subsequent cyclic voltammetry.

2. Materials and Methods

2.1 Surface treatments

Commercial pure titanium (Ti > 99.5%, Nilaco Co., Japan) was cut into rectangular 10 × 10 × 1 mm^3 samples, abraded with #400 diamond plates, washed with acetone, 2-propanol and ultrapure water in ultrasonic cleaner for a period of 30 min, and then dried at 40 °C. These samples were soaked in 5 ml of a 5 M NaOH aqueous solution at 60 °C for 1h. After removal from the solution, they were gently rinsed with ultrapure water for 30 s. The treated samples were subsequently soaked in 10 ml of a 0.5 mM HCl solution at 40 °C for 3 h, washed with ultrapure water and dried immediately under nitrogen (N_2) gas flow to prevent a color heterogeneity on the sample surfaces. They were heated to 650 °C at a rate of 2.5 °C /min, maintained for 1 h, followed by cooling at a rate of 2.5 °C /min to ambient temperature under air or 99.999% N_2 gas flow with 1.5 L/min in an atmosphere furnace (MS-1871, Motoyama Co. Ltd., Osaka, Japan).

For the heat treatment with N_2 gas, the samples were placed in a tailored reaction chamber consisting of an alumina vessel with a 1 mm in diameter hole connected to a porous Ti filter, as shown in Figure 2, in order to reduce the oxygen contamination in the N_2 gas, which had been found to be 0.8 ppm by gas chromatography.

2.2 Ferrocene modification treatment

As a redox active compound, we used 1,1'-ferrocenylbis(phosphonic acid), 1,1'-Fc[P(O)(OH)$_2$]$_2$, , prepared according to a reported method[14]. The modification of the 1,1'-ferrocenylbis(phosphonic acid) on the electrodes was performed as follows: an electrode and 1-mM EtOH solution of 1,1'-ferrocenylbis(phosphonic acid) were placed in a vial and its opening was closed with a rubber septum. The vial was filled with high-purity argon gas (99.999%) for 30 min. Then, the vial opening was quickly closed by an aluminum seal, then immersed in an oil bath and heated 48 h at 120°C. After heating, the vial was to room temperature and the electrode taken out of the liquid phase and is washed with EtOH several times, then used for the reflection spectrum and CV determination.

2.3 Surface analyses

2.3.1 Scanning electron microscopy.

The surfaces and cross-sections of the Ti metal samples subjected to the chemical and heat treatments were coated with a Pt/Pd film and observed under field-emission scanning electron microscopy (FE-SEM; S-4300, Hitachi Co., Japan) at a voltage of 15 kV.

2.3.2 Thin film X-ray diffraction and Raman spectrometry.

The surface of the Ti metal samples subjected to the chemical and heat treatments were analyzed using thin film X-ray diffraction (TF-XRD; RNT-2500, Rigaku Co., Japan) employing a CuKα X-ray source operating at 50 kV and 200 mA. The glancing angle of the incident beam was set to an angle of 1º against the sample surface. The Raman profiles of the samples were collected using a Fourier transform confocal laser Raman spectrometer (FT-Raman; LabRAM HR800, Horiba Jovin Yvon, France) at a wavelength of 514.5 nm and using an Ar^+ laser at a laser power of 16 mW.

2.3.3 Scratch resistance measurement.

The scratch resistance of the surface layer that was formed on the treated Ti metal samples by the chemical and heat treatments was evaluated by measuring the critical load by which the layer was detached from the substrate using a thin-film scratch tester (CSR-2000, Rhesca Co., Japan) that employed a stylus with a diameter of 5 mm and a spring constant of 200 g mm^{-1}. Based on the data in the JIS R-3255 standard, the amplitude, scratch speed and loading rate used were 100 μm, 10 μm s^{-1} and 100 mN min^{-1}, respectively. Five measurements were carried out for each sample, and the average value was used in the analysis.

2.3.4. X-ray photoelectron spectroscopy.

The surfaces of the Ti metal samples subjected to the chemical and heat treatments were analyzed using X-ray photoelectron spectroscopy (XPS; ESCA-3300KM, Shimadzu Co., Japan). In this analysis, MgKα radiation (λ = 9.8903A˚) was used as the X-ray source. The XPS take-off angle was set at 45º, which enabled the system to detect photoelectrons to a depth of 5–10 nm from the surface. The binding energies of the measured spectra were calibrated with reference to the C1s peak of the surfactant CH_2 groups on the substrate at 284.6 eV. The measured spectra were decomposed and subjected to curve fitting for quantitative analysis.

2.3.5. Radio frequency (RF) glow discharge optical emission spectroscopy.

The depth profiles of various elements on the surface of the Ti metal samples subjected to the NaOH, HCl and heat treatments in N_2 atmosphere were analyzed using RF glow discharge optical emission spectroscopy (GD-OES; GD-Profiler 2, Horiba Co., Japan) under Ar sputtering at an Ar pressure of 600 Pa. An RF electric field with a power of 35W was applied at a regular interval of 20 ms.

2.3.6. Electrical resistance measurements.

The surface of the Ti metal sample subjected to the chemical and heat treatments was partially polished so as to expose a certain area of the metal surface. A silver (Ag) sheet of 5 × 5 mm^2 was pasted on the unpolished area by hydrophobic conductive glue. It was confirmed by cross-sectional SEM observation that there was no penetration of the glue into the metal substrate. Ag wires were attached both on the Ag sheet and the polished area by the conductive glue, and the electrical resistance between them was measured with a two-terminal method using a potentiostat (HZ-5000, Hokuto Denko Co., Tokyo, Japan).

2.3.7. Fourier transform infrared spectroscopy.

The Fourier transform infrared (FTIR) profiles of the Ti metal samples before and after ferrocene modification were collected using a Fourier transform infrared spectrometer (FTIR; BioRad FTS575) a surface reflectance measurements unit.

2.3.8. Surface area measurement.

Ti metal plates having 20 × 5 × 1 mm^3 were prepared for surface area measurement. Ten samples subjected to the chemical and heat treatments were placed in a volumetric gas adsorption measurement instrument (Belsorp18, BEL Japan INC., Osaka, Japan) and their total surface area was measured by recording the Kr adsorption–desorption isotherms. The relative ratio of the measured surface area to the theoretical flat area of the metal samples was calculated by dividing the former by the latter, and the result was used for analysis.

2.4. Cyclic voltammetry

Cyclic voltammetry was measured with AUTOLAB model PGSTAT128N under the following conditions; in a 0.1M KNO_3 solution, the modified electrode was used as a WE, Pt foil as a CE, and Ag/AgCl as an RE. CV data were taken at scan rate 100 mVs^{-1} under Ar atmosphere.

3. Results

3.1 Surface structures

Figure 3 shows the FE-SEM photographs of the surfaces and cross-sections of the Ti metal, both untreated and subjected to the NaOH, HCl and heat treatments. A fine network structure on a nanometer scale formed on the surface of the metal after the initial NaOH treatment. This was unchanged by the subsequent HCl treatment, but was slightly sintered by the heat treatment in air or N_2 atmosphere. It is evident from the cross-sectional view that the network is approximately 600 nm in thickness and composed of many feather-like phases that are elongated perpendicular to the surface. The density of the surface layer increased with increasing depth. The surface area measurement revealed that the surface area of the Ti metal subjected to NaOH and HCl treatments was 5.70×10^{-2} m^2/g, 103 times larger than that of the theoretical flat surface (S_0). This value was decreased to 0.72×10^{-2} m^2/g (13 times larger than S_0) or 3.46×10^{-2} m^2/g (63 times larger than S_0) when the metal was subsequently heat-treated in air or N_2 atmosphere.

Table 1 shows the result of the XPS quantitative analysis of the surface of the Ti metal subjected to the NaOH, HCl, and heat treatments. The NaOH treatment incorporated 5.7 % of Na ions onto the surface of the metal. The Na ions were completely removed by the subsequent HCl treatment. When the treated Ti metal was heat treated in air, it showed only a contamination-derived N1s peak at 400 eV in binding energy [15,16]. In contrast, 0.4 % of the peak at 396 eV, which was assigned to Ti-N bonding[15,16], appeared on the surface of the metal in addition to the peak at 400 eV when the metal was heat treated in N_2 atmosphere instead of air. The presence of Ti-N bonding can be confirmed on the XPS profiles of N 1s on the treated metal as shown in Figure 4. This shows that some amount of nitrogen was incorporated into the surface layer by the heat treatment in the N_2 atmosphere. In contrast, Ti 2p spectrum shows the peaks at 459 and 464 eV, which were assigned to Ti-O bonding[17], but does not clearly show the peak at 455 eV attributed to Ti-N bonding[17] probably due to its small intensity.

Figure 5 shows the TF-XRD and FT-Raman profiles of the surface of the Ti metal that was untreated and subjected to the NaOH, HCl and heat treatments. The broad FT-Raman peaks occurring around 280, 450, 700, 820 and 910 cm^{-1} in wave number appeared after the NaOH treatment, and they were assigned to sodium hydrogen titanate, $Na_xH_{2-x}Ti_3O_7$[9,13]. When the sample was subsequently soaked in HCl solution, the intensity of the TF-XRD peak occurring at around 28 degrees in 2θ and the Raman peak occurring at around 910 cm^{-1} in wave number decreased, indicating that the sodium hydrogen titanate had transformed into hydrogen titanate, $H_2Ti_3O_7$[9,13], as a result of the exchange of the sodium ions for oxonium ions. The hydrogen titanate was transformed into anatase- and rutile-type TiO_2 by the heat treatment in air, while TiN, TiN_xO_{1-x}[18], Ti_2N and anatase, accompanied by a small amount of Ti_4O_7[19] were formed on the surface of the Ti metal as the result of the heat treatment in N_2 atmosphere.

Figure 6 shows the depth profile of the GD-OES spectra of the Ti metal subjected to the NaOH, HCl, and heat treatments in N_2 atmosphere. It can be seen from Figure 6 that N was detected mainly in the deeper region of the metal and comparatively

slightly in the upper layer. A gradual decrease of H and O, and gradual increase of Ti that was observed from the surface to the metal substrate indicates that a graded structure in terms of the chemical composition was formed by the chemical and heat treatments.

Figure 7 shows the scratch resistance of the Ti metal subjected to the NaOH, HCl and heat treatments. The scratch resistance of the surface layer that formed as the result of the initial NaOH treatment was as low as 7 mN. This low scratch resistance was unchanged by the subsequent HCl treatment, but was increased markedly, to 100 or 70 mN, by the final heat treatment in air or N_2 atmosphere.

3.2. Electrical conductivity

Table 2 shows the results of the electrical resistance measurement and electrical conductivity calculated by the following equation (1).

$$\sigma = \frac{A}{R} \quad (1)$$

Where σ is the electrical conductivity, A the cell constant and R the electrical resistance. The cell constant (A) is defined as A = L/S, using the length (L) and area (S) of the material. In the present study, L and S correspond to the thickness of the surface layer and the contact area between the surface network layer and the conductive glue under the electrode made of the Ag-sheet.

The contact area of the conductive glue to the surface layer is estimated as that between the theoretical flat surface and the actual surface area of the sample obtained experimentally by gas adsorption assessment. It is shown in Table 2 that the electrical conductivity of the metal after the NaOH and HCl treatments was estimated to be $1.5 \times 10^{-7} \sim 1.5 \times 10^{-5}$ mho cm^{-1}, which is in the range of a semiconducting material. It significantly decreased to $2.9 \times 10^{-13} \sim 3.8 \times 10^{-12}$ mho cm^{-1}, which is in the range of an insulating material, as a result of the heat treatment in air. In contrast, it slightly increased to $4.1 \times 10^{-7} \sim 2.6 \times 10^{-5}$ mho cm^{-1} by the heat treatment in N_2 atmosphere.

3.3. Surface modification with 1,1'-ferrocenylbis(phosphonic acid)

Figure 8 shows the FTIR spectra of the Ti metal surface subjected to the NaOH, HCl and heat(N_2) treatments, and subsequently subjected to ferrocene modification. It is shown in Figure 8 that a large peak around 1080 cm^{-1}, which is attributed to a P-O-Ti bond[6] , appeared on the surface of the metal after the ferrocene treatment, indicating that the 1,1'-ferroocenylbis(phosphonic acid) were chemically bonded though their terminal phosphate groups with the surface oxide layer formed on the metal.

3.4. Cyclic voltammetry

Figure 9 shows the result of cyclic voltammetry (CV) applied to the Ti metal subjected to the ferrocene modification following the NaOH, HCl and heat(N_2) treatments. A redox wave with peaks at approximately 0.26 and 0.43 V was observed on the treated metal (broken line). Its maximum current and potential difference were I_{max} = 1.4 mA and ΔE = 0.17 V,

respectively. In contrast, almost no electric current was observed on the chemical and heat treated Ti metal before the ferrocene modification (dot line). Ti metal without the chemical and heat treatments had no capacity for ferrocene fixation, and thus it showed almost no CV currents as the case of the chemical and heat treated Ti metal before ferrocene modification (data not shown).

4. Discussion

It is apparent from the experimental results that all of the preferable characteristics, such as the high specific surface area, electrical conductivity and large capacity for catalyst support, as well as a high degree of scratch resistance, were conferred on the Ti metal by the NaOH, HCl and heat treatments in the N_2 atmosphere. It should be noted that the heat treatment in air resulted in a significant decrease in electrical conductivity as shown in Table 2, and hence the treated metal was not useful as an electrode. The surface structural changes which took place in the Ti metal due to the chemical and heat treatments are similar to those in Figure 1.

A fine network layer approximately 600 nm in thickness was formed on the surface of the Ti metal by the NaOH treatment. This network consisted of nano-sized sodium hydrogen titanate, $Na_xH_{2-x}Ti_3O_7$. When the metal was soaked in HCl solution, the sodium hydrogen titanate substituted sodium ions with oxonium ions so as to form a hydrogen titanate, $H_2Ti_3O_7$, due to its layered structure [20]. Thus, the treated metal possessed a surface area that was 103 times larger than the theoretical flat surface.

When the metal was subsequently heat-treated in N_2 atmosphere, the hydrogen titanate was transformed into anatase and Ti_4O_7 accompanied by the induction of a small amount of nitrogen, as shown in Figure 5 and Table 1. TiN, TiN_xO_{1-x} and Ti_2N were formed in the deeper region of the surface layer, as seen in Figures 4, 5 and 6.

It was reported that Ti alloys such as Ti-6Al-4V and Ti-29Nb-13Ta-4.6Zr are easily oxidized by heat treatment, even in N_2 gas, with the contamination of several parts per million (ppm) of oxygen, since titanium has a higher affinity for oxygen than nitrogen[21]. The reaction of TiN with oxygen can be described using the following equation (2).

$$TiN + O_2 = TiO_2 + \frac{1}{2}N_2 \qquad (2)$$

According to thermodynamics data[22], the standard Gibbs free energy for formation of TiN and TiO_2 (rutile type) at 900 K are $\Delta G^{\circ}_{TiN(900K)}$ = -252.281 kJ mol^{-1}, and $\Delta G^{\circ}_{TiO2(900K)}$ = -780.233 kJ mol^{-1}, respectively. The equilibrium oxygen partial pressure between TiO_2 and TiN at 900 K was calculated using following equation, under the assumption that the pressure of N_2 is approximately equal to 1 atm, and the activity coefficients of TiN and TiO_2 are 1.

$$\ln P_{O_2} = \frac{\Delta G^{\circ}_{TiO_2(900K)} - \Delta G^{\circ}_{TiN(900K)}}{RT} \qquad (3)$$

Where R = 8.314 × 10^{-3} kJ mol^{-1} K^{-1} is the gas constant and T the absolute temperature.

As a result of the substituting above values in equation (3), $P_{O2} = 2.28 \times 10^{-31}$ atm is obtained. This means that TiN can be oxidized in the atmosphere in which the oxygen partial pressure is higher than 2.28×10^{-31} atm.

When the oxygen partial pressure is lower than the equilibrium oxygen partial pressure described above, it is considered that reverse reaction of equation (2) proceeds, meaning nitrogen dope into titanium oxides. In order to achieve the low oxygen

partial pressure and to increase reaction rate, severe conditions such as NH_3 atmosphere and high temperatures of 800-1000 ºC are usually used for a nitrogen dope on titanium oxide powders[23,24].

In the present study, some amount of nitrogen was incorporated into the surface layer of the chemically treated Ti metal, and even the oxygen-deficient titanium oxide Ti_4O_7 was formed by the heat treatment with the mild conditions of N_2 atmosphere and temperature of 650 ºC. These phenomena may be explained as follows. Since a porous Ti metal disc was used as the oxygen getter and set in the reaction chamber as shown in Figure 2, the supplied N_2 gas could not pass thorough the porous disc without giving its contaminated oxygen. As a result, the oxygen partial pressure in the reaction chamber might be reduced close to that of the equilibrium oxygen partial pressure described above. Furthermore, the oxygen in the surface layer diffuses into the metal substrate during the course of the heat treatment due to its gradient chemical composition, as shown in Figure 6. It is assumed that the low crytalline hydrogen titanate prepared by NaOH and HCl treatments has amounts of active sites to form Ti-N bondings. A TEM study revealed that nitrogen-doped and defective titanium oxides were tend to be formed in the top of the surface layer, whereas TiN_xO_{1-x} and Ti_2N were formed in the bottom[25]. Although the specific surface area of the metal was somewhat decreased by the heat treatment, it was still 63 times larger than that of the theoretical flat surface. The decrease in the specific surface area might be due to the sintering of the surface layer during the heat treatment, as seen in Figure 3.

It is known that the electrical conductivity of TiO_2 is as low as that of insulating materials, but it is increased markedly, up to the range of 10^{-2} to 10 mho cm^{-1}, by the induction of a small degree of oxygen deficiency and/or nitrogen [26-28]. Therefore, the relatively high electrical conductivity of the Ti metal after the heat treatment in the N_2 atmosphere in the present study is due to the formation of oxygen-deficient titanium oxide, such as the Ti_4O_7 resulting from nitrogen induction as well as Ti_2N, TiN_xO_{1-x} and TiN in the surface layer. Since the estimated electrical conductivity of the surface titanium oxide layer in the present study was $4.1 \times 10^{-7} \sim 2.6 \times 10^{-5}$ mho cm^{-1} , which is still lower than that of the reported value [29,30], a further increase in electrical conductivity is expected by increasing the amount of the oxygen deficiency and/or doped nitrogen in the surface titanium oxide layer. In contrast, when the metal was heat-treated in air instead of N_2, neither the induction of nitrogen into titanium oxides nor the formation of titanium nitrides was observed as shown in Figure 5, and Table 1. As a result, the electrical conductivity of the metal treated in this manner was as low as that of an insulating material, as shown in Table 2.

It was reported that titanium oxides immobilize various types of catalyst that have been functionalized with carboxyl or phosphate groups[5,6]. In the present study, the capacity for catalyst support by the metal after the heat treatment in N_2 atmosphere following the NaOH and HCl treatments was estimated by utilizing ferrecene, that is widely used for CV due to its stable redox property. The ferrocene molecules were functionalized with phosphate groups to form 1,1'-ferrocenylbis(phosphonic acid) and used in the ferrocene modification. As a result, they were successfully immobilized on the treated metal by forming a Ti-O-P bond, as shown in Figure 8. It is expected that the treated Ti metal can also immobilize other catalysts, such as the Ru complex [1] and Mn porphyrin system[2] that enhance efficiency of electrolysis of water, if they are similarly functionalized with phosphate groups.

When the ferrocene-modified Ti metal prepared in this manner was subjected to CV measurement, it displayed a high electrical current of 1.4 mA but with 0.17 V of potential variation. Xiao et al. observed a similar value of potential differences

of ~0.16 V on a TiO_2 nano tube (TNT) electrode that was prepared by anodizing and subsequent annealing in N_2 atmosphere[31]. This higher electrical conductivity is an advance, since the observed potential differences were a little higher than the 0.059 V of the theoretical value[32]. Further study to increase the electrical conductivity of the metal is currently in progress.

5. Conclusions

A new type of Ti metal electrode with one-dimensional titanium oxide surface layer doped with nitrogen and oxygen deficiency was produced by the NaOH, HCl and heat treatment in N_2 atmosphere. Its electrical conductivity was estimated to be $4.1 \times 10^{-7} \sim 2.6 \times 10^{-5}$ mho cm^{-1}, which is in the range of a semiconducting material. The metal had a high specific surface area that was 63 times larger than the theoretical flat surface and exhibited a high degree of scratch resistance. Furthermore, it successfully immobilized 1,1'-ferrocenylbis(phosphonic acid) on its surface so as to induce a high electric current on the performance of CV. It is expected that a metal treated in this manner would be able to immobilize various types of catalyst and thus potentially be useful as an electrode in various electrochemical systems.

Acknowledgements

This work was financially supported by Elemental Science and Technology Project, MEXT, JST ACT-C, and Grant-in-Aid for Scientific Research (A) (#23245035, YN).

References

1 J. A. Gilbert, D. S. Eggleston, W. R. Murphy Jr, D. A. Geselowitz, S. W. Gersten, D. J. Hodgson, T. J. Meyer, J. Am. Chem. Soc. 1985, 107, 3855-3864.

2 Y. Naruta, M. Sasayama, T. Sasaki, Angew. Chem. Int. Ed. Engl. 1994, 33, 1839-1841.

3 D. Fattakhova-Rohlfing, M. Wark, T. B. Brezesinski, B. M. Smarsly, J. Rathousky, Adv. Funct. Mater. 2007, 17, 123-132.

4 S. J. Bao, Q. L. Bao, C. M. Li, Z. L. Dong, Electrochem. Commun. 2007, 9, 1233-1238.

5 T. H. Tran, A. Y. Nosaka, Y. Nosaka, J. Photochem. Photobiol. A Chem. 2007, 192, 105-113.

6 S.-M. Chang, C.-Y. Hou, P.-H. Lo, C.-T. Chang, Appl. Catal. B: Environ. 2009, 90, 233-241.

7 D. Wang, T. Hu, L. Hu, B. Yu, Y. Xia, F. Zhou, W. Liu, Adv. Funct. Mater. 2009, 19, 1930-38.

8 H.-M. Kim, F. Miyaji, T. Kokubo, S. Nishiguchi, T. Nakamura, J. Biomed. Mater. Res. 1999, 45, 100-107.

9 X. Sun, Y. Li, Chem. Eur. J. **2003**, 9, 2229-2238

10 S. Yamaguchi, H. Takadama, T. Matsushita, T. Nakamura, T. Kokubo, J. Ceram. Soc. Japan **2009**, 117, 1126-1130.

11 K. Kawanabe, K. Ise, K. Goto, H. Akiyama, T. Nakamura, A. Kaneuji, T. Sugimori, T. Mtsumoto, J. Biomed. Mater. Res. B Appl. Biomater. **2009**, 90, 476-481.

12 M. Uchida, H.-M. Kim, T. Kokubo, S. Fujibayashi, T. Nakamura, *J. Biomed. Mater. Res. Appl. Biomater.* **2002**, *63*, 522-530.

13 T. Kawai, T. Kizuki, H. Takadama, T. Matsushita, H. Unuma, T. Nakamura, T. Kokubo, *J. Ceram. Soc. Japan* **2010**, *118*, 19-24.

14 S.R. Alley, W. Henderson, *J. Organometallic. Chem.*, **2001**, *637-639*, 216-229.

15 N.C. Saha, H.G. Tompkins, *J. Appl. Phys.* **1992**, *72*, 3072-3079.

16 National Institute of Standards and Technology (NIST) database.

17 NIST X-ray Photoelectron Spectroscopy Database, Version 4.1.

18 I. M. Pohrelyuk, V. M. Fedirko, O. I. Yas'kiv, D. B. Lee, O. V. Tkachuk, *Mater. Sci.* **2009**, *45*, 779-789.

19 Joint Committee on Powder Diffraction Standards (JCPDS) Powder Diffraction Data File 01-071-1428.

20 E. Jr Morgado, M. A. S. de Abreu, O. R. C. Pravia, B. A. Marinkovic, P. M. Jardim, F. C. Rizzo, A. S. Arou´jo, *Solid State Sci.* **2006**, *8*, 888-900.

21 M. Nakai, M. Niinomi, T. Akahori, N. Ohtsu, H. Nishimura, H. Toda, H. Fukui, M. Ogawa, J. Japan Inst. Metals. 2007, 71, 415.

22 I. Barin, in Thermochemical Data of Pure Substances. VCH, Weinheim, New York, 1989.

23 F. Tessier, C. Zollfrank, N. Travitzky, H. Windsheimer, O. Merdrignac-Conanec, J. Rocherulle, P Greil, J. Mater. Sci. 2009, 44, 6110-6116.

24 T. H. Tran, A. Y. Nosaka and Y. Nosaka, J. Photochem. Photobiol. A: Chem., 2007, 192, 105-113.

25 R. Khanna, S. Yamaguchi, A. Valanezhad, T. Kokubo, T. Matsushita, Y. Naruta and H. Takadama, J. Mater. Chem. A, 2014, 2, 1809-1817.

26 T. Ma, M. Akiyama, E. Abe, I. Imai, *Nano lett.* **2005**, *5*, 2543-47.

27 H. Tang, K. Prasad, R. Sanjinbs, P. E. Schmid, F. Levy, *J. Appl. Phys.* **1994**, *75*, 2042-47.

28 L. Forro, O. Chauvet,D. Emin, L. Zuppiroli, H. Berger, F. Levy, *J. Appl. Phys.* **1994**, *75*, 633-665.

29 P. Xiao, Y. Zhang, B. B. Garcia, S. Sepehri, D. Liu, G. Cao, *J. N. N.* **2008**, *8*, 1-11.

30 J. Wang, in *Analytical Electrochemistry.* John Wiley & Sons, New Jersey, **2000**, Ch. 2.

Figure captions

Figure 1 Structural changes of the surfaces of Ti metal due to NaOH, HCl and heat treatments.

Figure 2 Reaction chamber for heat treatment in N_2 atmosphere

Figure 3 FE-SEM photographs of the surfaces and cross-section of Ti metal untreated and subjected to NaOH and HCl treatments, and subsequent heat treatment in air or N_2 atmosphere.

Figure 4 XPS profiles of N 1s and Ti 2p spectra on Ti metal subjected to heat treatment in N_2 atmosphere following NaOH and HCl treatments.

Figure 5 TF-XRD and FT-Raman profiles of the surfaces of Ti metal untreated and subjected to NaOH and HCl treatments, and subsequent heat treatment in air or N_2 atmosphere.

Figure 6 GD-OES depth profiles of the surfaces of Ti metal subjected heat treatment in N_2 atmosphere following NaOH and HCl treatments.

Figure 7 Scratch resistance of Ti metal subjected to NaOH, HCl and heat treatments.

Figure 8 FTIR spectra of Ti metal (a) without or (b) with ferrocene modification treatment following NaOH, HCl and heat treatment in N_2 atmosphere.

Figure 9 CV curve of Ti metal with ferrocene modification treatment following NaOH, HCl and heat treatment in N_2 atmosphere; Ferrocene treated (solid line) and before ferrocene modification (broken line).

Table1 XPS quantitative analysis of surface layers of Ti metal untreated and subjected to NaOH and HCl treatments, and subsequent heat treatment in air or N_2 atmosphere.

Treatment	C_{1s}%	O_{1s}%	N_{1s}%		Na_{1s}%	Ti_{2p}%
			396 eV	400 eV		
Untreated	16.1	58.7	UD	1.7	UD	23.5
NaOH	8.5	62.9	UD	0.2	5.7	22.7
NaOH-HCl	11.8	63.6	UD	1.4	UD	23.3
NaOH-HCl-heat(air)	13.7	61.6	UD	0.3	UD	24.4
NaOH-HCl-heat(N_2)	16.7	59.3	0.4	0.4	UD	23.1

UD:under detection

Treatment	Electrical resistance / Ω	Cell constant / cm^{-1}	Electrical conductivity /mho cm^{-1}
NaOH-HCl	15.7	$2.3 \times 10^{-6} \sim 2.4 \times 10^{-4}$	$1.5 \times 10^{-7} \sim 1.5 \times 10^{-5}$
NaOH-HCl-heat(air)	3.3×10^{6}	$1.8 \times 10^{-5} \sim 2.4 \times 10^{-4}$	$2.9 \times 10^{-13} \sim 3.8 \times 10^{-12}$
NaOH-HCl-heat(N_2)	9.2	$3.8 \times 10^{-6} \sim 2.4 \times 10^{-4}$	$4.1 \times 10^{-7} \sim 2.6 \times 10^{-5}$

Table2 Electrical conductivity of Ti metal subjected to NaOH and HCl treatments, and subsequent heat treatment in air or N_2 atmosphere.

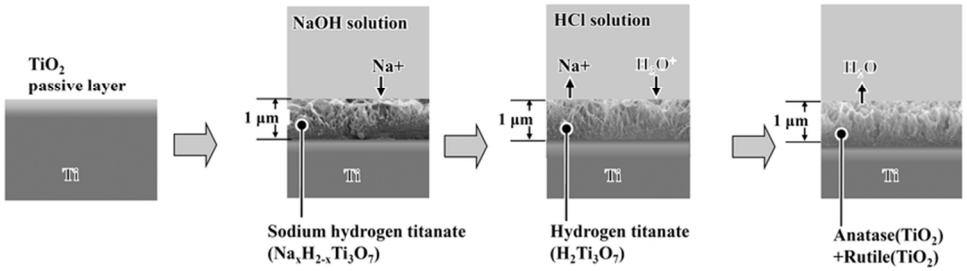

Figure 1
76x22mm (300 x 300 DPI)

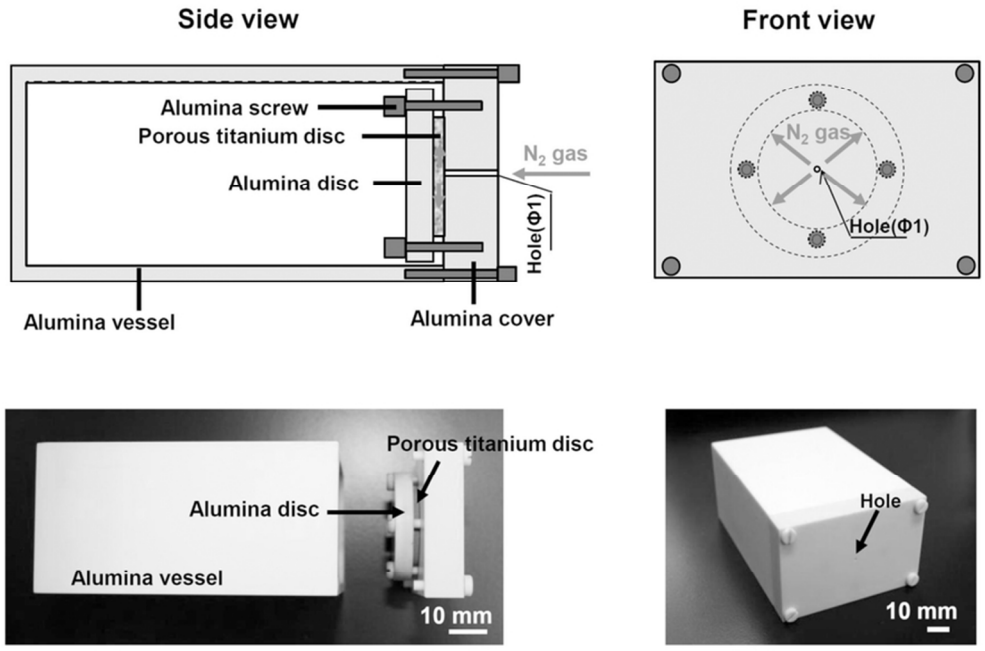

Figure 2
76x51mm (300 x 300 DPI)

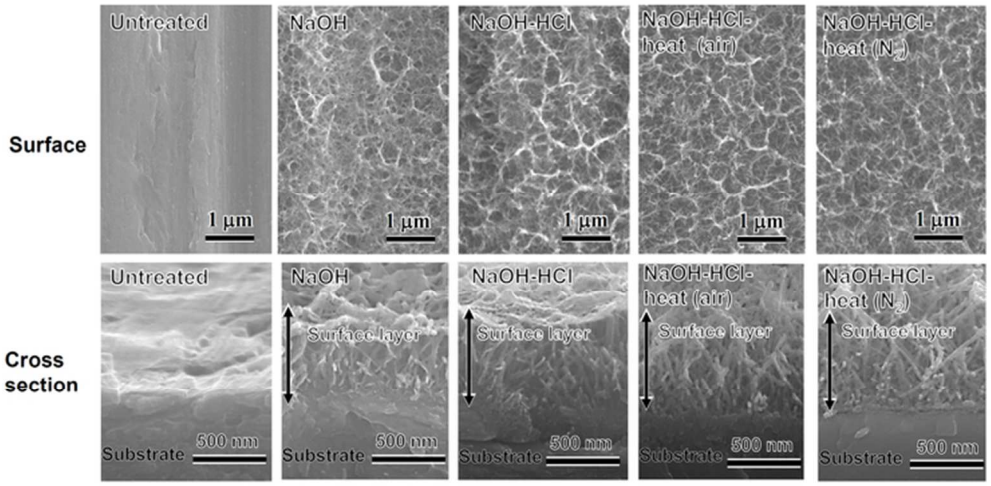

Figure 3
63x31mm (300 x 300 DPI)

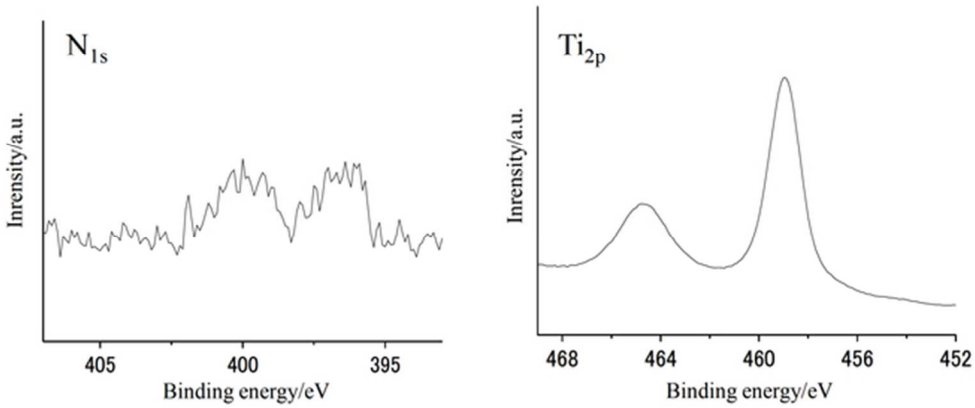

Figure 4
56x25mm (300 x 300 DPI)

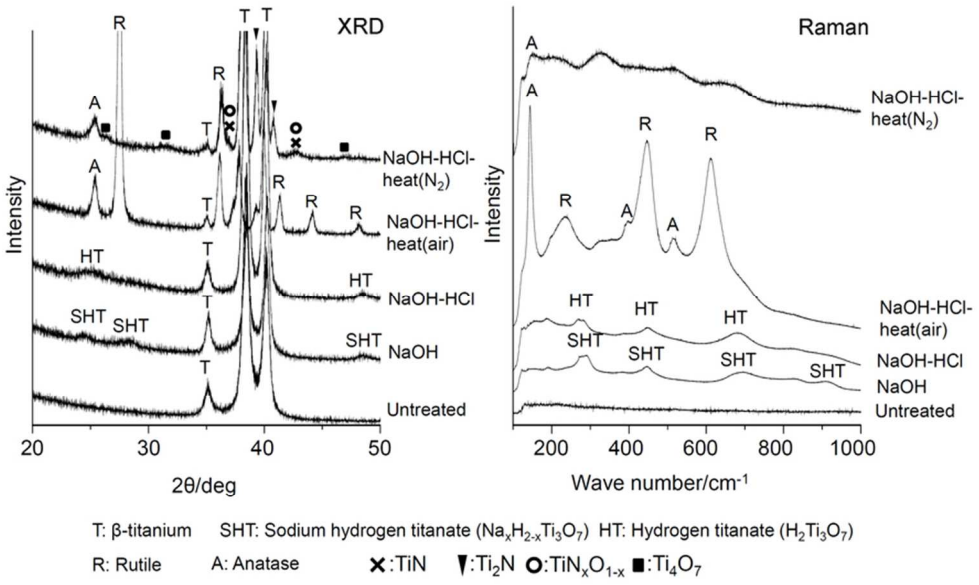

Figure 5
76x46mm (300 x 300 DPI)

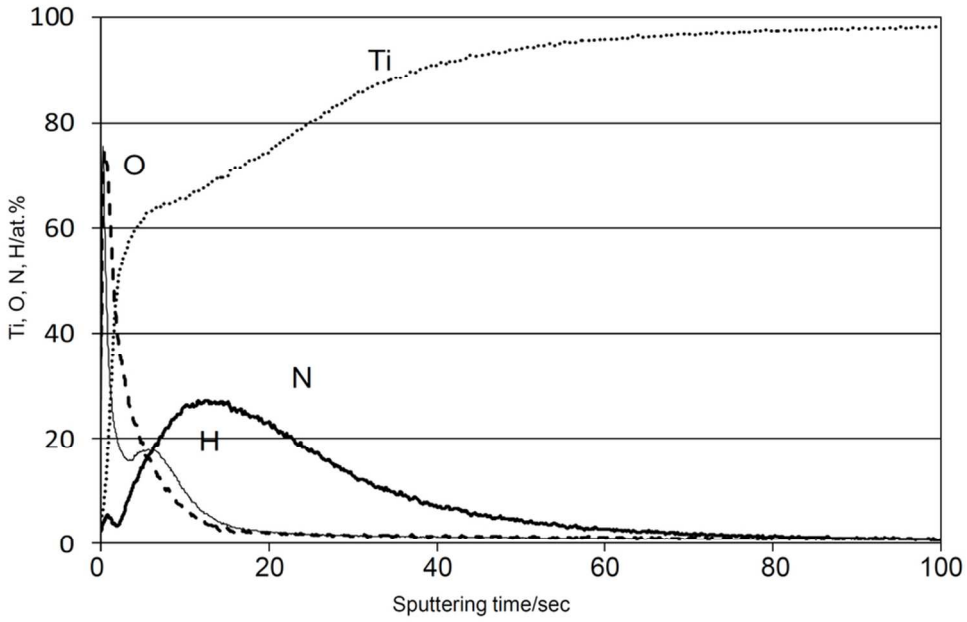

Figure 6
84x54mm (300 x 300 DPI)

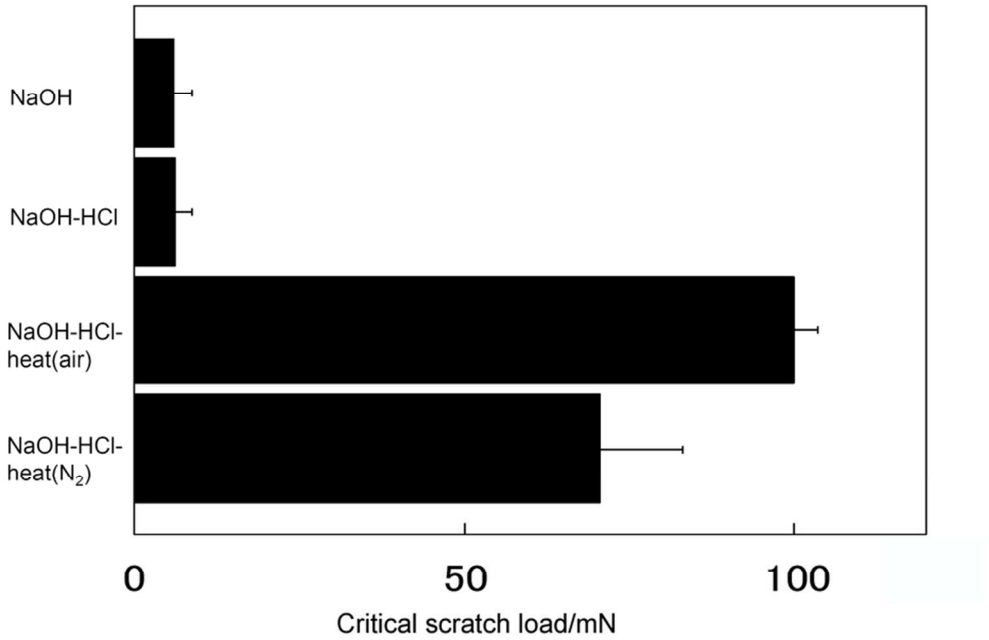

Figure 7
79x53mm (300 x 300 DPI)

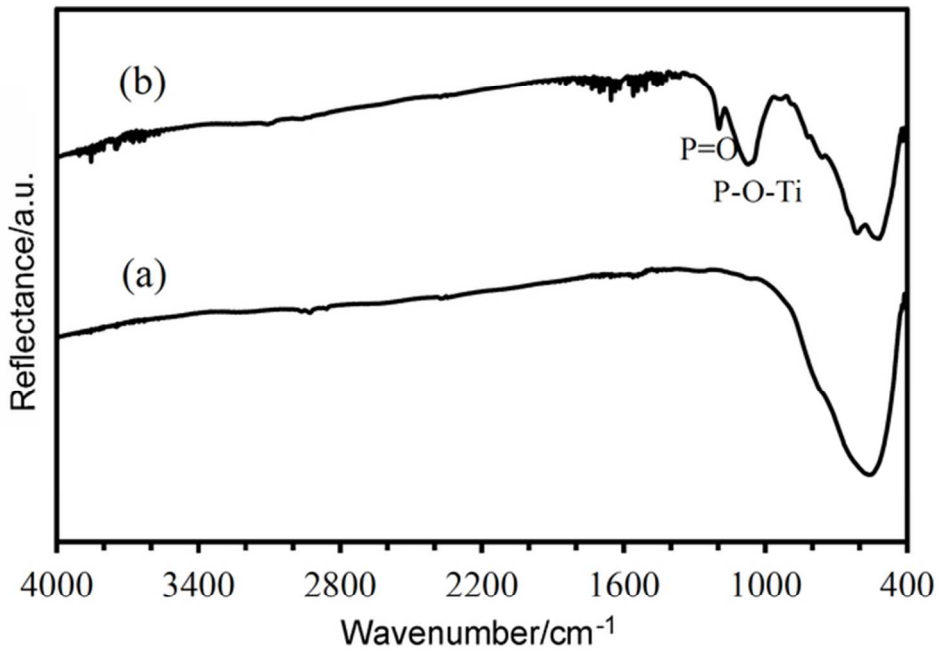

Figure 8
59x42mm (300 x 300 DPI)

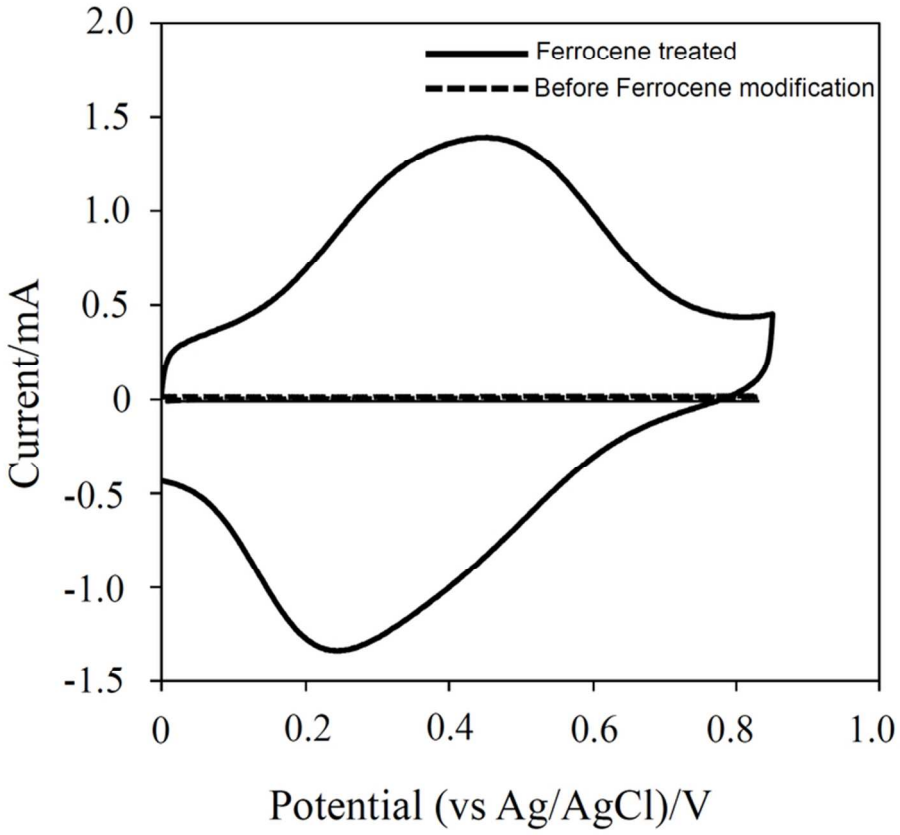

Figure 9
73x67mm (300 x 300 DPI)